Appl. Phys. A (2016) 122:383
DOI 10.1007/s00339-016-9866-4

Applied Physics A
Materials Science & Processing

CrossMark

Ion beam lithography with gold and silicon ions

Gediminas Seniutinas[1,2] · Armandas Balčytis[1,2] · Yoshiaki Nishijima[3] · Achim Nadzeyka[4] · Sven Bauerdick[4] · Saulius Juodkazis[1,2]

Received: 17 August 2015 / Accepted: 14 November 2015 / Published online: 14 March 2016
© Springer-Verlag Berlin Heidelberg 2016

Abstract Different ion species deliver a different material sputtering yield and implantation depth, thus enabling focused ion beam (FIB) fabrication for diverse applications. Using newly developed FIB milling with double charged Au^{2+} and Si^{2+} ions, fabrication has been carried out on Au-sputtered films to define arrays of densely packed nanoparticles supporting optical extinction peaks at visible-IR wavelengths determined by the size, shape, and proximity of nanoparticles. Results are qualitatively compared with Ga^{+} milling. A possibility to use such ion implantation to tailor the etching rate of silicon is also demonstrated.

1 Introduction

The advancement in fields of manufacturing various micro/nanodevices highly depends on available fabrication techniques. Metamaterial surfaces [1, 2], planar optical elements [3, 4], plasmonic circuits [5, 6] and many other fields are moving forward as higher-resolution and higher-throughput technologies evolve. Mask projection UV lithography with achievable resolutions below 100 nm [7] is used where high throughput is required, i.e., the mass production and large-area devices. UV lithography requires a mask with a pattern to be projected on a desired substrate. The masks are usually created using higher spatial resolution (below 10 nm), but relatively slower electron beam lithography (EBL) where focused high-energy (30–100 keV) electrons are scanned to locally modify a resist layer for subsequent metallization and liftoff or etching. The bottleneck in mask fabrication using EBL is caused by nanoscale focus and large write-field, and the drawback is overcome only by industrial multi-beam and projection setups. For patterns which combine large-area low-resolution and small-footprint high-resolution patterns, for example, in terahertz antennas, a combination of photolithography and EBL is a common choice [8].

These two major micro/nanofabrication techniques can be further complimented by focused ion beam (FIB) lithography, which has an additional capability beyond resist exposure and can be used for material removal and a surface 3D milling with tens-of-nanometers resolution. Milling with Ga^{+}-ions is the most mature technique in the field of focused ion beam technology and is mostly used for obtaining sample cross sections and lamella preparation for transmission electron microscopy. Ion beam stability issues have limited FIB applications in high-resolution patterning over large areas, but significant progress has been achieved over the last decade, and now systems with resolutions down to 10 nm are commercially available. Low melting temperature and relatively heavy Ga ions made this material attractive in the design of FIB systems. However,

✉ Gediminas Seniutinas
GSeniutinas@swin.edu.au; gdseniutinas@gmail.com

Saulius Juodkazis
SJuodkazis@swin.edu.au

1 Centre for Micro-Photonics, Faculty of Science, Engineering and Technology, Swinburne University of Technology, Hawthorn, VIC 3122, Australia

2 Melbourne Centre for Nanofabrication, Australian National Fabrication Facility, Clayton, VIC 3168, Australia

3 Department of Electrical and Computer Engineering, Graduate School of Engineering, Yokohama National University, 79-5 Tokiwadai, Hodogaya-ku, Yokohama 240-8501, Japan

4 Raith GmbH, Konrad-Adenauer-Allee, 8, 44263 Dortmund, Germany

for many plasmonic applications Ga implantation and deposition into gold significantly increases optical losses at the visible-IR spectral range where Au nanostructures are widely used to concentrate light into "hot spots" for various applications, e. g., surface-enhanced Raman scattering (SERS) [9, 10], second harmonic generation (SHG) [11, 12] and enhanced fluorescence [13]. Arrays of plasmonic nanoparticles can also realize all-optical switching via cross-polarization control of the optical extinction via coupling due to shape, alignment and separation of nanoparticles [5, 14], a very appealing for fast telecommunications. Modification of micro/nanoelectrical circuits using direct write is very attractive for rapid prototyping; however, Ga implantation creates electrical shorts in the circuits and decreases overall performance of the modified devices. As gold and silicon are widely used in plasmonics and electronics, respectively, the use of Au and Si ions in FIB systems is expected to enable new devices and faster prototyping processes. Recently developed Au/Si and Au/Ge alloys have been implemented as ion sources[15], allowing for high-resolution patterning with single or double charged Au, Si or Ge ions. Highly precise deposition of metals opens possibility for fabrication of high-aspect-ratio X-ray optical elements [16].

Here we demonstrate the direct write capabilities for creating metal nanoparticle arrays using double charged Au and Si ions. The measured optical properties of the patterns indicate variations of resonance positions for similar structures fabricated using diverse ion species. Direct surface modification/functionalization with Au^{2+} is also demonstrated.

2 Experimental

Ion beam milling using Ga^{+}, Si^{2+} and Au^{2+} ions was carried out on gold-coated glass substrates. The substrates were prepared by first cleaning 1 cm $\times$ 1 cm and 500 µm thick BK7 glass pieces in an ultrasonic bath using acetone and methanol followed by drying in nitrogen flow. Then, 3-nm chromium for adhesion and 50-nm gold layers were e-beam evaporated (J.K. Lesker, AXXIS). The coated substrates were subsequently nanopatterned using FIB with multi-ion species (IonLiNE, Raith). Single charged Ga and double charged Au/Si ions were further used for direct writing of nanoparticle arrays into the evaporated gold film.

Etching experiments were conducted using a single-side-polished p-type $\langle 100 \rangle$ orientation silicon wafer as a substrate. The wafer was rinsed in methanol to remove any remaining particles and dried under gentle nitrogen flow. The substrate was then loaded for gold implantation by FIB.

3 Results and Discussion

As mentioned in the introduction, many applications use plasmonic particles where localized surface plasmon (LSP) resonance results in the enhancement of electromagnetic field in particular spots around the structure. The resonance frequency can be tuned by changing the particle shape [17], material [18, 19], size or by altering its environment [20]. Gold bars ranging in size from tens to a few hundred nanometers were shown to exhibit LSP resonances at the visible-IR spectral range [21, 22], thus lasers can be used for resonant excitation. Most of the practical plasmonic devices such as SERS or SHG substrates use dense arrays of resonant particles to achieve a higher signal which is accumulated over a large area as opposed to a single particle response. Large nanoparticle arrays can be coated by nonlinear polymers [23, 24] to enhance harmonics generation further.

Most of the periodic plasmonic substrates are prepared using a top-down approach and, since high-resolution patterns are required, EBL is typically used. Electron beam lithography process involves many resist handling steps and is time-consuming in terms of finding optimal exposure conditions, especially in R&D applications where various geometries need to be tested. We used a fairly straightforward approach to fabricate tens-of-microns sized fields of plasmonic nanoparticles by direct writing using FIB. Therefore, the resist processing steps are eliminated in direct write FIB and writing speeds up to 10^3 μm^2/hour can be reached when using Ga^{+} ions [25]. The FIB system used here has a vertical column and is similar to a standard R&D EBL tools. Ion beam lithography is still an emerging field and, in principle, patterning speeds comparable or even higher than EBL could be reached [26, 27]. Noteworthily, FIB can also be used for resist exposure and requires much less dose as ions are heavier, hence it allows faster writing time.

Direct FIB milling is especially appealing where high-density nanoparticle arrays at tens-of-nanometers resolution need to be fabricated. Figure 1 shows a 25 µm by 25 µm field patterned with focused Ga^{+} beam. The two particle geometries are 90-nm-diameter disks (Fig.1a) and 90 nm $\times$ 210 nm rectangles (Fig.1b). In both cases, neighboring particles are separated by a 90-nm gap. All structures used in our experiments were written by drawing a grid composed of 25 µm long perpendicular single-pixel lines on the gold coating. The particle size was controlled by changing the distance between the parallel lines, and the separation width has been varied by altering the ion beam current. Higher currents would result in higher material removal rates, though at the cost of a wider groove.

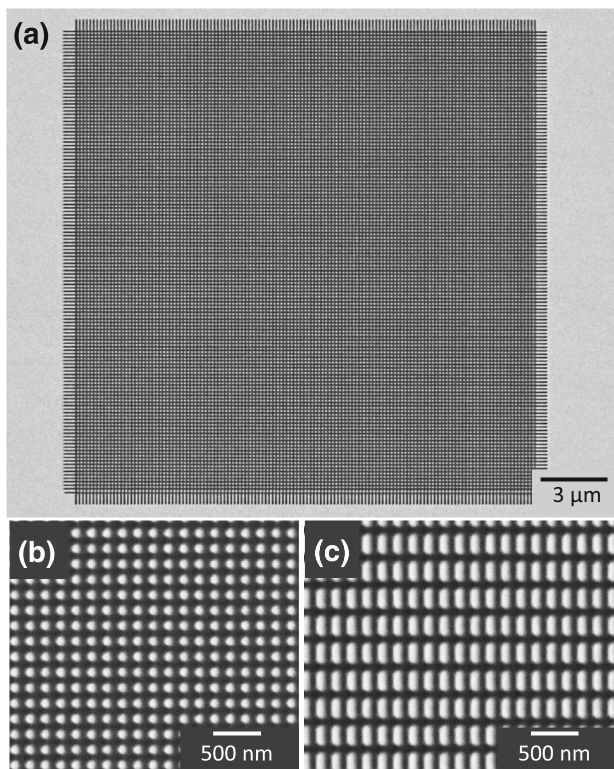

Fig. 1 **a** 25 µm by 25 µm field nanoparticle array directly milled using focused Ga ions. The structure was patterned by writing mesh perpendicular lines into the evaporated gold layer; **b** and **c** close-up SEM images of the obtained disk and rectangle arrays, respectively

The extinction spectra of Ga milled patterns were measured using a broadband unpolarized illumination source. Transmission through the nanoparticle patterned area, T, and reference transmission through the substrate, T_0, was measured and extinction was calculated as $Ext = -lg(T/T_0)$. The resulting experimental data are plotted in Fig.2. No distinctive plasmon resonance peaks were observed for the disk structures in our measurement window. However, the bar-shaped particles exhibited a broad resonance at around 850 nm wavelength. This resonance is well suited for SERS measurements as laser wavelengths around 750–800 nm are often used for Raman excitation.

As the rectangular geometry Ga^+ ion milled particle arrays have showed the plasmonic resonance peak, the design was further considered for fabrication with double charged gold and silicon ions. Gold is heavier than gallium, and due to double charge the accelerated ions have higher energy, thus, the material sputtering rate for Au^{2+} is three time higher when compared to Ga^+. On the other hand, silicon is significantly lighter and even though its ions also have a 2+ charge, the milling rate is roughly three times lower when compared to Ga^+. Scanning electron

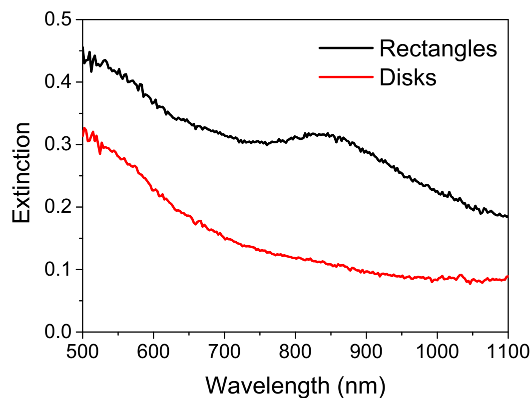

Fig. 2 Extinction spectra of the FIB-milled disk and rectangle arrays. The excitation was measured under an unpolarized broadband illumination and detection

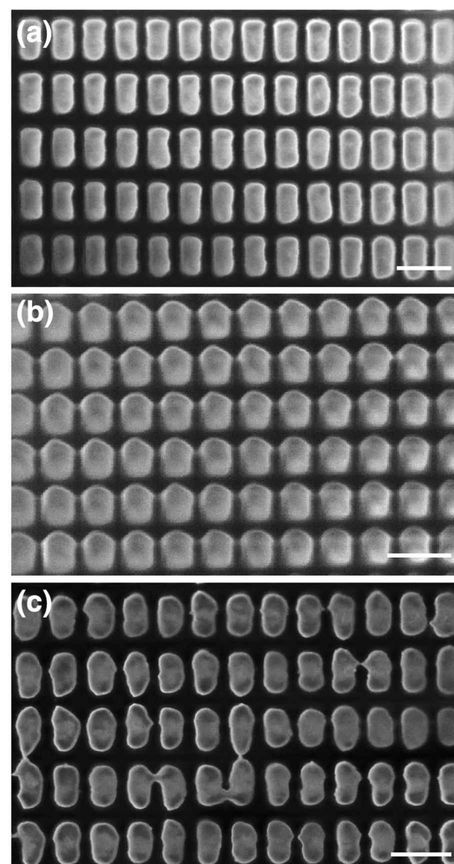

Fig. 3 Array of rectangular nanoparticles with dimensions 190 nm × 100 nm and a ~50 nm spacing. **a** and **b** are respectively top and 45 degree tilted view SEM images of Au^{2+} milled pattern; **c** top view of Si^{2+} ion milled structure. *Scale bars* are 250 nm in length

micrographs of the patterned structures are shown in Fig. 3. A slightly different nanoparticle array writing approach was chosen when using Au^{2+} than in the case of milling with Ga^+. It was found that the heavier Au^{2+} ions result in

enhanced redeposition of the milled gold film; hence, if the perpendicular line patterns are milled in two sequential steps, gold re-sputtered in the second step tends to close the perpendicular interparticle gaps milled in the previous step. The writing strategy was then adjusted to first mill vertical lines with only half the dose required to puncture the gold film, then write horizontal ones at full dose, and finally repeat the half dose single pass on the vertical lines. As can be noticed by comparing Fig. 3a, c images, the particle edges are sharper and the geometry is better maintained when milling with heavier Au ions rather than with lighter Si. However, slightly slanted walls are also obtained most probably due to beam wings.

Extinction spectra from the Au^{2+}-patterned nanoparticle arrays were measured using an aberration corrected IsoPlane SCT 320 (Princeton Instruments) spectrograph mounted on a side port of Eclipse Ti-U (Nikon) microscope and is shown in Fig. 4. The measurements were done using a polarized light source, thus the longitudinal resonance (when light polarization is parallel to the longer edge of the particle) is well expressed in the spectra and is shown to have a quality factor of $Q = wavelength/width \simeq 5$, i.e., the ratio of the central resonant *wavelength* and the spectral *width* at the full width half maximum (FWHM). Gold layer milling using gold ions apparently has small effect on optical extinction as the same material is implanted. However, for actual sensor applications when high light intensity is at the skin depth in subsurface regions and for masking applications in chemical/plasma etching, a shallowly implanted Au ions and their modification of surrounding crystalline lattice might have influence and should be better understood.

Controlled implantation of Au into the substrate near the end points of an antenna structure where light is concentrated might be useful for SERS-based sensors. Further studies are required to find out if gold ions implanted into a substrate can be activated for functionalization. Application

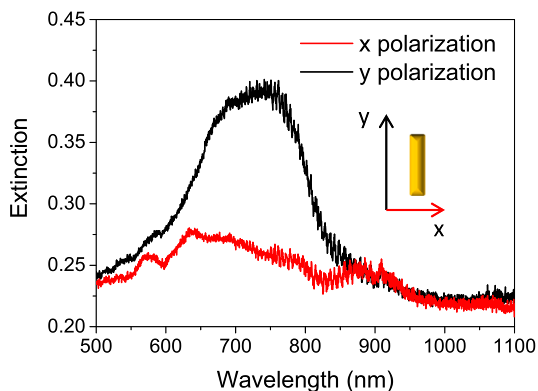

Fig. 4 Measured extinction spectra of the nanoparticle array shown in Fig.3a. The spectra were measured for two perpendicular polarizations as shown in the inset, the resonance peak at around 750 nm represents the longitudinal plasmon oscillation mode

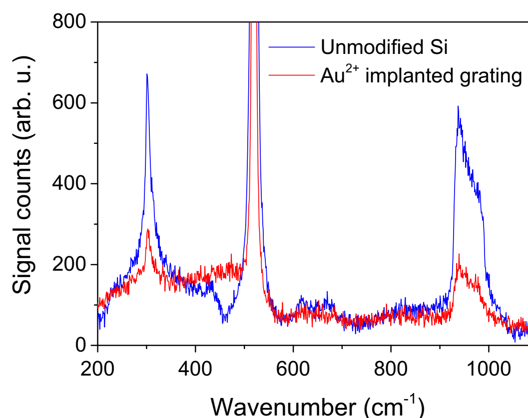

Fig. 5 Raman spectra obtained from Au^{2+} implanted and unmodified silicon before plasma etching. 785 nm wavelength was used to excite the sample

of selective gold implantation was demonstrated to write arbitrary graphene patterns on silicon carbide substrate [28]. It was shown that gallium implanted into Si or diamond surfaces forms a several nanometer thick hard mask for etching [29, 30]. A possibility to alter the silicon etching rate using high lateral precision Au implantation was tested. A grating pattern was written on a silicon wafer (single side polished, p-type, $\langle 100 \rangle$) using a focused Au^{2+} beam resulting in the implanted ion density of $10^{15} - 10^{16}\,\mathrm{ions/cm^2}$. Raman spectra measured from the exposed and unmodified silicon regions are depicted in Fig. 5. The modified areas show decreased silicon second-order phonon peak intensities at around 300 and 900–1000 $\mathrm{cm^{-1}}$ possibly due to reduced density of phononic excitations due to lattice damage by the ions [31]. However, no change in the full width at half maximum nor shift in spectral position of the peaks occur and this means that initial crystalline structure is maintained over the bulk of the substrate [31], the only noticeable spectral difference characteristic of amorphized silicon is the lower energy side tail of 520 $\mathrm{cm^{-1}}$ peak. This is reasonable as the ion penetration depth is tens of nanometers and the used excitation wavelength of 785 nm probes over a substrate depth of several micrometers, thus the damaged volume contributes to the signal significantly less than the undamaged Si bulk.

The implanted silicon substrate was etched using SF_6/O_2 gas mixture in Samco RIE-101iPH etcher. Figure 6a shows SEM images of the substrate before and after the plasma treatment. A 300-nm width nanograss lines separated by 100 nm wide flat silicon areas were observed after the etching (Fig. 6). High energy (30 kV acceleration voltage) Au ions break silicon bonds and make it more reactive [32], thus increasing the etching rate. The nanograss in the damaged areas was formed possibly due to additional local masking of the implanted ions. Actual line

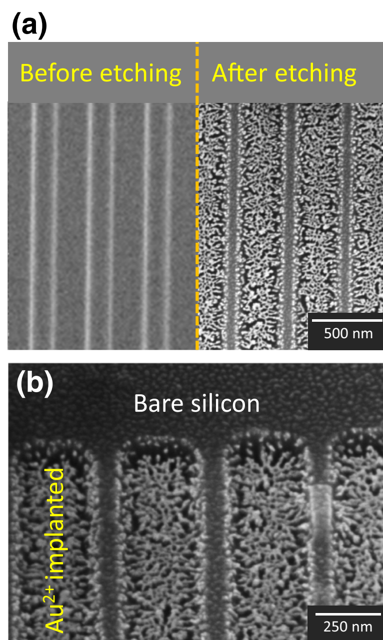

Fig. 6 Silicon surface after 30-s etching in SF_6/O_2 plasma. The ion implanted regions resulted in nanograss formation. **a** top view; **b** close up 45 degree view

widths after the etching were $\sim$50 nm larger as compared to FIB patterned ones. This is probably due to ions in the beam wings as their dose was too low to cause noticeable surface modification but high enough to create the masking effect. Hence, further investigation is needed to better understand nanograss formation when FIB masking is used.

High precision implantation on insulating substrates, like diamond or SiC, is challenging as surface charging shifts the beam during writing and distorts the final pattern. In that case, UV light illumination of the patterning area might be used to effectively neutralize surface charging [33] and allow for nanoscale precision.

SERS measurements using thiophenol as a test analyte were carried out for the Au milled as well as for Au implanted Si substrates using standard procedure [34, 35]. Due to covalent bonding of thiols to Au there was expectation that SERS signals from nanoclusters of Au implanted near the antenna tips or from the surface will be distinguished. However, only very weak SERS was observed in those first trials. Au antennas for the 785 nm wavelength used in SERS should be optimized and different Au^{+} and Au^{2+} ions compared for milling and implantation.

4 Conclusions

Focused ion milling (or ion beam lithography) with increasing variety of ion species is becoming a promising nanotechnology tool and is not limited to sample slicing for TEM lamella preparation. High-density nanoparticle arrays with a footprint of 25-by-25 µm were fabricated using focused Ga^{+}, Au^{2+} and Si^{2+} ions. The milling rate for Au^{2+} was evaluated to be almost one order of magnitude higher than for Si^{2+} and 3 times greater than using Ga^{+} ions.

Precise high energy Au^{2+} implantation into silicon allows to change Si etching rate and tailor surface morphology at the nanoscale. The 400-nm period and 300-nm-width Si nanograss lines were demonstrated by gold implantation and subsequent dry etching. Milling, implanting of ions with a sub-100 nm resolution is expected to open new applications in the fields of nanotechology. Since different eutectic alloys especially with gold can be prepared, this technology using multi-ion sources is promising as it can be readily extended into material nanoprocessing with wide range of ions.

Acknowledgments We acknowledge support by ARC Linkage LP120100161 and Discovery DP130101205, DP120102980 grants. SJ acknowledge a startup funding of Nanotechnology facility by Swinburne University of Technology.

References

1. F. Garcia-Vidal, L. Martin-Moreno, J. Pendry, Surfaces with holes in them: new plasmonic metamaterials. J. Opt. A: Pure Appl. Opt. **7**(2), S97 (2005)
2. X. Shen, T.J. Cui, Ultrathin plasmonic metamaterial for spoof localized surface plasmons. Laser Photon. Rev. **8**(1), 137–145 (2014)
3. Z. Liu, J.M. Steele, W. Srituravanich, Y. Pikus, C. Sun, X. Zhang, Focusing surface plasmons with a plasmonic lens. Nano Lett. **5**(9), 1726–1729 (2005)
4. P. Genevet, N. Yu, F. Aieta, J. Lin, M.A. Kats, R. Blanchard, M.O. Scully, Z. Gaburro, F. Capasso, Ultra-thin plasmonic optical vortex plate based on phase discontinuities. Appl. Phys. Lett. **100**(1), 013101 (2012)
5. T.J. Davis, D.E. Gómez, F. Eftekhari, All-optical modulation and switching by a metamaterial of plasmonic circuits. Opt. Lett. **39**(16), 4938–4941 (2014)
6. A.M. Funston, C. Novo, T.J. Davis, P. Mulvaney, Plasmon coupling of gold nanorods at short distances and in different geometries. Nano Lett. **9**(4), 1651–1658 (2009)
7. N. Mojarad, J. Gobrecht, Y. Ekinci, Beyond EUV lithography: a comparative study of efficient photoresists performance. Sci. Rep **5**(9235) (2015)
8. G. Seniutinas, G. Gervinskas, E. Constable, A. Krotkus, G. Molis, G. Valušis, R.A. Lewis, S. Juodkazis, THz photomixer with milled nanoelectrodes on LT-GaAs. Appl. Phys. A **117**(2), 439–444 (2014)
9. Y. Nishijima, J.B. Khurgin, L. Rosa, H. Fujiwara, S. Juodkazis, Randomization of gold nano-brick arrays: a tool for SERS enhancement. Opt. Express **21**(11), 13502–13514 (2013)
10. R. Buividas, P.R. Stoddart, S. Juodkazis, Laser fabricated ripple substrates for surface-enhanced Raman scattering. Annalen Physik **524**(11), L5–L10 (2012)
11. R. Czaplicki, H. Husu, R. Siikanen, J. Mäkitalo, M. Kauranen, J. Laukkanen, J. Lehtolahti, M. Kuittinen, Enhancement of second-

harmonic generation from metal nanoparticles by passive elements. Phys. Rev. Lett. **110**(9), 093902 (2013)
12. R. Czaplicki, J. Mäkitalo, R. Siikanen, H. Husu, J. Lehtolahti, M. Kuittinen, M. Kauranen, Second-harmonic generation from metal nanoparticles: Resonance enhancement versus particle geometry. Nano Lett. **15**(1), 530–534 (2014)
13. R.M. Bakker, H.-K. Yuan, Z. Liu, V.P. Drachev, A.V. Kildishev, V.M. Shalaev, R.H. Pedersen, S. Gresillon, A. Boltasseva, Enhanced localized fluorescence in plasmonic nanoantennae. Appl. Phys. Lett. **92**(4), 043101 (2008)
14. Y. Nishijima, J.B. Khurgin, L. Rosa, H. Fujiwara, S. Juodkazis, Tunable Raman selectivity via randomization of a rectangular pattern of nanodisks. ACS Photonics **1**(10), 1006–1012 (2014)
15. S. Bauerdick, L. Bruchhaus, P. Mazarov, A. Nadzeyka, R. Jede, Multispecies focused ion beam lithography system and its applications. J. Vac. Sci. Technol. B **31**(6), 06F404/1-5 (2013)
16. C. Chang, A. Sakdinawat, Ultra-high aspect ratio high-resolution nanofabrication for hard X-ray diffractive optics. Nature Comm. **5**, 4243 (2014)
17. W.A. Murray, W.L. Barnes, Plasmonic materials. Adv. Mat. **19**(22), 3771–3782 (2007)
18. P.R. West, S. Ishii, G.V. Naik, N.K. Emani, V.M. Shalaev, A. Boltasseva, Searching for better plasmonic materials. Laser Photon. Rev. **4**(6), 795–808 (2010)
19. Y. Nishijima, Y. Hashimoto, G. Seniutinas, L. Rosa, S. Juodkazis, Engineering gold alloys for plasmonics. Appl. Phys. A **117**(2), 641–645 (2014)
20. K.L. Kelly, E. Coronado, L.L. Zhao, G.C. Schatz, The optical properties of metal nanoparticles: the influence of size, shape, and dielectric environment. J. Phys. Chem. B **107**(3), 668–677 (2003)
21. H.J. Huang, C.-P. Yu, H.C. Chang, K.P. Chiu, H. Ming Chen, R.S. Liu, D.P. Tsai, Plasmonic optical properties of a single gold nano-rod. Opt. Express **15**(12), 7132–7139 (2007)
22. E.K. Payne, K.L. Shuford, S. Park, G.C. Schatz, C.A. Mirkin, Multipole plasmon resonances in gold nanorods. J. Phys. Chem. B **110**(5), 2150–2154 (2006)
23. G. Seniutinas, R. Tomašiūnas, R. Czaplicki, B. Sahraoui, M. Daškevičienė, V. Getautis, Z. Balevičius, Arylmethylene-1, 3-indandione based molecular glasses: Third order optical nonlinearity. Dyes Pigm. **95**(1), 33–40 (2012)
24. G. Navickaitė, G. Seniutinas, R. Tomašiūnas, R. Petruškevičius, V. Getautis, M. Daškevičienė, Photoinduced orientational dynamics of azophenylcarbazole molecules in polycarbonate. Dyes Pigm. **92**(3), 1204–1211 (2012)
25. G. Seniutinas, G. Gervinskas, A. Balčytis, F. Clark, Y. Nishijima, A. Krotkus, G. Molis, G. Valušis, S. Juodkazis, Nanoscale precision in ion milling for optical and terahertz antennas. In: SPIE OPTO. International Society for Optics and Photonics, pp. 93 740P–93 740P (2015)
26. C.R. Marrian, D.M. Tennant, Nanofabrication. J. Va. Sci. Technol. A **21**(5), S207–S215 (2003)
27. M. Malinauskas, A. Žukauskas, S. Hasegawa, Y. Hayasaki, V. Mizeikis, R. Buividas, S. Juodkazis, Ultrafast laser processing of materials: from science to industry. Light: Sci. Appl. (2015) (in press)
28. S. Tongay, M. Lemaitre, J. Fridmann, A. Hebard, B. Gila, B. Appleton, Drawing graphene nanoribbons on SiC by ion implantation. Appl. Phys. Lett. **100**(7), 073501 (2012)
29. N. Chekurov, K. Grigoras, A. Peltonen, S. Franssila, I. Tittonen, The fabrication of silicon nanostructures by local gallium implantation and cryogenic deep reactive ion etching. Nanotechnology **20**(6), 065307 (2009)
30. W. McKenzie, J. Pethica, G. Cross, A direct-write, resistless hard mask for rapid nanoscale patterning of diamond. Diamond Related Mater. **20**(5), 707–710 (2011)
31. G. Sahu, Confinement in MeV Au2+ implanted Si: a Raman scattering study. Adv. Nat. Sci.: Nanosci. Nanotechnol. **5**, 015002 (2014)
32. R. Charavel, J.-P. Raskin, Tuning of etching rate by implantation: Silicon, polysilicon and oxide. In: Ion Implantation Technology: 16th International Conference on Ion Implantation Technology-IIT 2006, vol. 866, no. 1. AIP Publishing, pp. 325–328 (2006)
33. G. Gervinskas, G. Seniutinas, S. Juodkazis, Control of surface charge for high-fidelity nanostructuring of materials. Laser Photon. Rev. **7**(6), 1049–1053 (2013)
34. G. Gervinskas, G. Seniutinas, J.S. Hartley, S. Kandasamy, P.R. Stoddart, N.F. Fahim, S. Juodkazis, Surface-enhanced Raman scattering sensing on black silicon. Annalen Physik **525**(12), 907–914 (2013)
35. G. Seniutinas, G. Gervinskas, R. Verma, B.D. Gupta, F. Lapierre, P.R. Stoddart, F. Clark, S.L. McArthur, S. Juodkazis, Versatile SERS sensing based on black silicon. Opt. Express **23**(5), 6763–6772 (2015)